

Evaluation of a miniature electromagnetic position tracker

Johann Hummel,^{a)} Michael Figl, Christian Kollmann, and Helmar Bergmann^{b)}
*Department of Biomedical Engineering and Physics, General Hospital, University of Vienna,
Währinger Gürtel 18–20, A-1090 Vienna, Austria*

Wolfgang Birkfellner

*CARCAS-group, University Hospital of Basle, Switzerland, and the Department of Biomedical Engineering
and Physics at General Hospital Vienna, Austria*

(Received 23 January 2002; accepted for publication 30 July 2002; published 6 September 2002)

The advent of miniaturized electromagnetic digitizers opens a variety of potential clinical applications for computer aided interventions using flexible instruments; endoscopes or catheters can easily be tracked within the body. With respect to the new applications, the systematic distortions induced by various materials such as closed metallic loops, wire guides, catheters, and ultrasound scan heads were systematically evaluated in this paper for a new commercial tracking system. We employed the electromagnetic tracking system AuroraTM (Mednetix/CH, NDI/Can); data were acquired using the serial port of a PC running SuSE Linux 7.1 (SuSE, GmbH, Nürnberg). Objects introduced into the digitizer volume included wire loops of different diameters, wire guides, optical tracking tools, an ultrasonic (US) scan head, an endoscope with radial ultrasound scan head and various other objects used in operating rooms and interventional suites. Beyond this, we determined the influence of a C-arm fluoroscopy unit. To quantify the reliability of the system, the miniaturized sensor was mounted on a nonmetallic measurement rack while the transmitter was fixed at three different distances within the digitizer range. The tracker was shown to be more sensitive to distortions caused by materials close to the emitter (average distortion error $13.6 \text{ mm} \pm 16.6 \text{ mm}$ for wire loops positioned at a distance between 100 mm and 200 mm from the emitter). Distortions caused by materials near the sensor (distances smaller than 100 mm) are small (typical error $2.2 \text{ mm} \pm 1.9 \text{ mm}$). The C-arm fluoroscopy unit caused considerable distortions and limits the reliability of the tracker (distortion error $18.6 \text{ mm} \pm 24.9 \text{ mm}$). Distortions resulting from the US scan head are high at distances smaller than about 100 mm from the emitter. The distortions also increase when the scan head is positioned horizontally and close to the sensor (average error $4.1 \text{ mm} \pm 1.5 \text{ mm}$ when the scan head is positioned within a distance of 100 mm from the sensor). The distortions are slightly higher when the ultrasound machine is switched on. We also evaluated the influence of common medical instruments on distance measurements. For these measurements the average deviation from the known distance of 200 mm amounted to $3.0 \text{ mm} \pm 1.5 \text{ mm}$ (undistorted distance measurement $1.5 \text{ mm} \pm 0.3 \text{ mm}$). The deviations also depend on the relative orientation between emitter and sensor. The results demonstrate that the miniature tracking system opens up new perspectives with regard to surgery applications where a flexible instrument is to be tracked within the body. Significant distortions caused by metallic objects only occur in the worst cases, for example, in the presence of a closed, unisolated wire loop or a C-arm fluorescence unit close to the emitter and which can be avoided by suitable usage. © 2002 American Association of Physicists in Medicine. [DOI: 10.1118/1.1508377]

Key words: magnetic tracking system, accuracy, computer aided surgery, frameless stereotaxy

I. INTRODUCTION

Image-guided or computer aided surgery (CAS) has witnessed constant development over the past decade. All surgical navigation systems are following the same basic setup. A sensor measures intraoperatively the position and orientation in the coordinate system of the patient, an imaging device or a surgical tool, and a computer correlates image data acquired pre- and intra-operatively through modalities like computed tomography (CT) or magnetic resonance imaging (MRI) to the intraoperative data. The usefulness of surgical navigation is fundamentally dependent on the accuracy and reliability of the tracking system. Optical tracking systems

(OTS) for position measurements provide the most reliable and precise position sensors available for medical applications.^{1–4} The restriction of this technology arises from the requirement of a free line-of-sight between the light emitting diodes (LED) and the camera assembly. Therefore only rigid instruments where the LED assembly is visible to the tracking system's camera at all times can be used. In a crowded operating field, requiring rigid instruments and the maintenance of line of sight to the instrument may further constrain the work of the surgeon.

Interventional applications using flexible instruments have to use other technologies for instrument tracking. Electromagnetic tracking system (EMTS) provide a possibility

for achieving this. Therefore, these devices have been used in CAS applications^{5,6} regardless of the fact that metallic ferromagnetic objects and stray fields from power lines can distort the acquired position data enormously. Referring to previous publications of our group^{7,8} and others,^{9,10} common commercial systems may exhibit inaccuracies between 1–15 mm and 1°–4° resulting from common surgical tools used inside the digitizer range of the EMTS. The calculation of position and orientation is based on the physical principle in that the systems are measuring either the induced voltage or the magnetic induction of an alternating current (ac) or direct current (dc) pulsed emitter. In consideration of this fact interference from conductive or ferromagnetic material is inevitable. Some improvement are achieved when the assembly is arranged in such a manner that the interfering object is placed outside the area between emitter and receiver.¹¹ In that case, the distortions are lower at the same emitter–sensor distance, and, under such conditions, good results were obtained using EMTS in CT-guided bronchoscopy,¹² three-dimensional ultrasonography,¹³ catheter positioning,¹⁴ and endoscopic surgery.¹⁵ According to Zaaroor *et al.*,⁵ an error of 5 mm would be acceptable for removing brain tumors of a size of 5 cm, but for functional neurosurgery or applications like navigating a guiding wire the accuracy has to be improved. For the successful application of navigation systems in interventional radiology, an accuracy in the range of 3–5 mm is desirable and the sensor should be small enough to be attached to the instruments. As opposed to optical tracking systems, the useful field-of-view is rather small. To overcome this limitation one can use an additional optical tracking system to navigate the field emitter of the EMTS. This would allow to move the emitter during the intervention since any movement of the emitter is registered and the new positions and angles of the electromagnetic sensor can be computed easily. This type of hybrid tracking system was described in an earlier paper of our group.²

Our motivation for using miniature sensors is to improve the navigation for endoscopes and guiding wires in interventional radiology and endosonography. Because of the poor image quality of ultrasonic images from an endoscopic US scan head it was deemed desirable to provide a slice of a pre-interventional CT or MR image with identical orientation and position as the intra-interventional US image to be overlaid with the latter. In case of positioning guiding wires we wanted to provide important reference slices, e.g., sagittal, coronal and axial, for identifying the current position of the instrument's tip inside the patient.

With regard to these aims we tested a newly developed 5 degree of freedom system which uses a proprietary iterative algorithm to determine the position of the sensor. The purpose of our experiments was to examine the influence on the accuracy of the system of

- (i) closed wire loops with different radii,
- (ii) guiding wires with different configurations of loops,
- (iii) US scan probes near to the emitter and the sensor,
- (iv) a mobile C-arm fluoroscopy unit,
- (v) optical tracking tools,

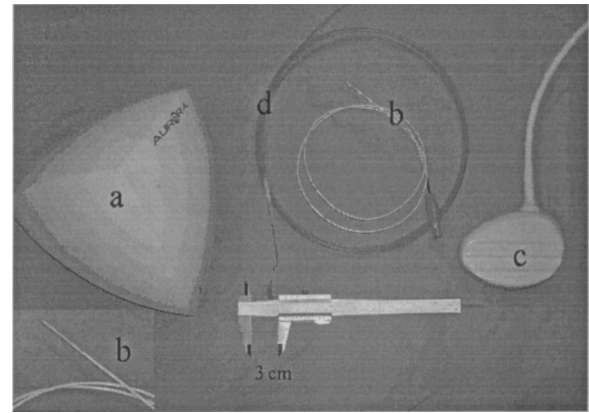


FIG. 1. The Aurora emitter (a) with a close-up of the sensor, (b), and some sources of distortion: the US scan head (c) and a guiding wire (d). Also shown is a caliper to indicate the size of the objects.

- (vi) an endoscope with a radial ultrasound scan head,
- (vii) a needle holder, biopsy forceps and a drill handle.

Supposing that these objects are representative for potential sources of distortion in our application we wanted to evaluate whether the tracking system used is suitable for navigational procedures. Since the C-arm fluoroscopy unit is the most important instrument of the interventional radiologist, we also included it in our list of disturbing objects.

II. MATERIALS AND METHODS

The tracking system under evaluation was the Aurora miniature electromagnetic tracking system (Mednetix/CH, NDI/Can, Fig. 1). Three degrees of freedom in position and two in angulation are provided. Specifications given by the manufacturer quote a positional accuracy of 1–2 mm and an angular accuracy of 1°–2° within the sensitive volume of 360 mm×600 mm×600 mm. The sensitive volume starts at a distance of 300 mm from the emitter. The tracking system employs a new proprietary iterative algorithm to determine the sensor's position and two angles. For the measurements we used an accurately machined nonmetallic table made of perspex, which was developed for previous evaluations.⁸ The setup is similar to that described there. In short, a metallic object representing the source of distortion is mounted on a sample holder that is mobile between receiver and sensor in the main plane (x and y coordinate) of the perspex table (Fig. 2). To allow for positioning of the object in the vertical direction (z coordinate) we used plastic boxes of different heights. During the measurements the metallic objects were moved in steps between the emitter and the sensor. The position indicated by the sensor is recorded for each step. The deviation is given by the difference between the positions recorded with and without the distorting object. For the distance measurements we calculated the euclidian distance between two sensor positions. During the measurements the whole system is placed on top of a wooden table and it was made sure that no other metallic object was to be found in

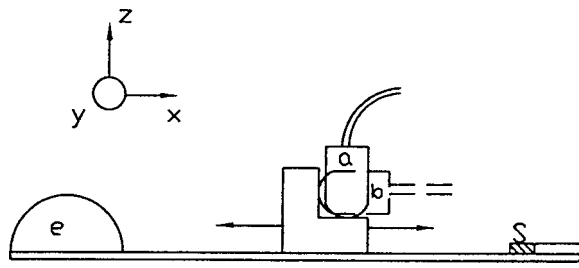


FIG. 2. A schematic illustration of the setup. The objects were mounted on the sample holder which can be moved in the x - y plane. In the illustration a US scan head is positioned upright (a) and horizontally (b). The emitter (e) and the sensor (s) are fixed on a wooden table. The shown coordinate system represents the coordinate system of the emitter.

the vicinity (approximately 1 m) of the emitter or the sensor. Various samples were employed as sources of distortion (Figs. 1 and 3).

A. Undistorted measurements and stylus calibration

The precision of the undistorted measurements was measured by calculating the mean value of 100 position data points each for several positions. The resulting mean values were compared with the specifications. The points used were at 300, 450, and 600 mm from the emitter in the horizontal plane.

To evaluate the accuracy for distance measurements, we measured distances between two markers positioned symmetrically with respect to the x axis on a measuring bar. The bar was positioned parallel to the y axis of the emitter coordinate system at a distance of 450 mm between emitter and bar. The tip of the sensor was placed at each marker and the positions indicated by the sensor were recorded. The resulting error was calculated as the difference between the Euclidian distance between the recorded sensor positions at the markers and the distance measured with a caliper, $\Delta = d_{\text{sensor}} - d_{\text{caliper}}$. We repeated these measurements for distances of 100 mm, 200 mm, 300 mm, 400 mm, and 500 mm between the markers.

In addition, we measured the accuracy of the location of the tip of a stylus by a method described by Hartov *et al.*¹⁶

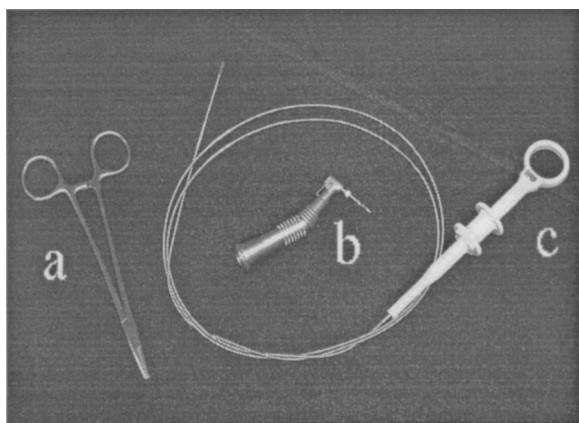


FIG. 3. Sources of distortions used for the distance measurements: a needle holder (a), a drill handle (b), and biopsy forceps (c).

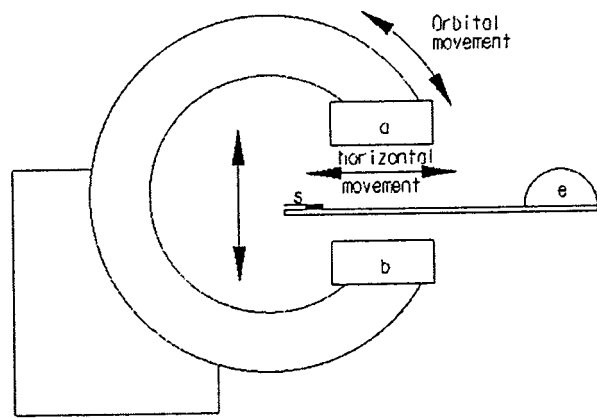
The calibrated value of the stylus tip position (i.e., the offset vector) was used to calculate the emitter coordinates of a given point. This was performed with 20 different orientations of the stylus. For all three coordinates the resulting standard deviation was calculated. The root mean square (rms) error was computed by

$$E_{\text{rms}} = \sqrt{\sigma_x^2 + \sigma_y^2 + \sigma_z^2}.$$

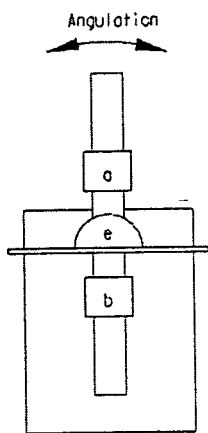
To examine the effect of sensor orientation, we measured an accurately known distance (obtained with a caliper) using the calibrated stylus. The position of the tip of the stylus was calculated as described by Hartov *et al.*¹⁶ The first position was measured holding the stylus upright, i.e., parallel to the z axis of the emitter coordinate system. The following position measurements were made at a marker at a distance of 20 cm. For these measurements the stylus was rotated by increments of 10 degrees around the x and the y axis, respectively. The deviation for each step was again calculated by $\Delta = d_{\text{stylus}} - d_{\text{caliper}}$ whereby d_{stylus} is the Euclidian distance between the calculated tip position of the first measurement and the calculated tip position obtained with the rotated stylus at the marker.

B. Influence of wire loops, guiding wires, and optical tracking tools

Three closed wire loops of copper with diameters of 30 mm, 100 mm, and 150 mm and thickness of 0.2 mm were used. For these measurements three distances between the emitter (i.e., field generator) and the sensor were used. Two were chosen close to the borders of the specified emitter volume (300 mm at the near border and 600 mm at the far border horizontally), and one in the middle (450 mm). The measurement space was divided into a 30 mm grid. For each sample 135 positions along the line connecting the emitter and sensor were measured for three different heights on the z axis. Furthermore, two different types of vascular wire guides, one made of stiff and another of flexible material with 150 cm length, bent to a loop with diameter of 150 mm, were used. All these loops were positioned with the spanning plane upright, i.e., perpendicular to the x - y plane of the emitter system. Additionally, active tracking sensors of two optical tracking systems (Polaris, Northern Digital Inc./Can, and Flashpoint 5000, Image Guided Technologies Inc./CO) in typical arrangements used in CAS were brought into the space between the emitter and sensor. For these measurements the distance between the sensor and the emitter was maintained at 450 mm. The distortions were measured by comparing the sensor readings (an average value of 100 measurements per point) taken with and without the metallic source of distortion in the digitizing volume. Position deviations were obtained by calculating the Euclidean distance between position values measured with and without the sources of distortion present. Angle measurements were not used in this study.



(a)



(b)

FIG. 4. (a) Orbital movement of the C-arm fluoroscopy unit. The emitter (e) and the sensor (s) are fixed on a wooden table. The labeled parts of the C-arm fluoroscopy units are the image intensifier (a) and the x-ray source (b). (b) Angulation of the C-arm fluoroscopy unit.

C. Influence of US scan head and a C-arm fluoroscopy unit

US scan head: To evaluate the effect, we mounted a scan head (C4-2, Ultramark 9, Advanced Technology Laboratories/USA) upright and horizontally on the sample holder (Fig. 2) and measured the distortion within an interval of 450 mm between emitter and detector.

C-arm fluoroscopy unit: All data were obtained with a Siremobil 2000 (Siemens/Erlangen, Germany) and with an interval of 450 mm between emitter and sensor. The parameter a in Fig. 11(a) gives the horizontal distance between the C-arm unit and the sensor. Positive values of a signify a horizontal translation towards the emitter. $a=0$ means that the x-ray source is positioned exactly below the sensor whereas a negative a indicates a horizontal translation of the C-arm further away from the emitter. To cover the range of possible C-arm positions we also rotated the arm around two different axes. Axis I corresponds to the C-arm orbital movement with a positive angle indicating a motion of the x-ray source towards the control unit of the C-arm [Fig. 4(a)]. Axis II corresponds to the C-arm angulation i.e., the rotation per-

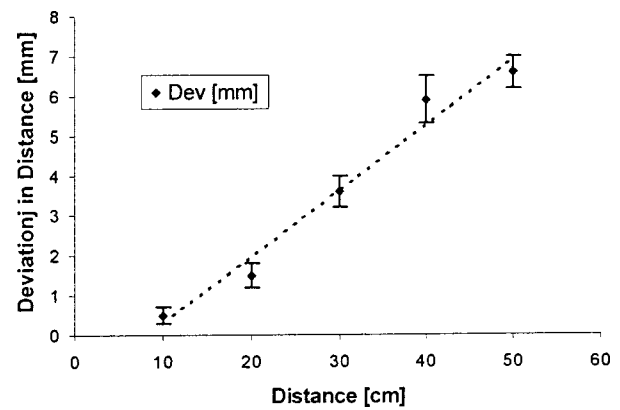


FIG. 5. Deviation resulting from the undistorted distance measurements with a linear regression shown as a dotted line. The mean value and the standard deviation obtained from the distance measurement of 20 cm was used for the figures showing the distorted distance measurements.

pendicular to the orbital rotation [Fig. 4(b)]. Here, positive values describe the clockwise movement of the image intensifier of the C-arm towards the emitter.

D. Distance measurements in the presence of distorting objects

We repeated the distance measurements described in Sec. II A with various objects between the emitter and the measuring bar. These sources of distortions were mounted on the sample holder which was moved along the x axis like for the wire loops. Figure 3 shows a drill, biopsy forceps, and a needle holder used for these measurements. Additionally, we employed a US scan head (C4-2, Ultramark 9, Advanced Technology Laboratories/USA) and an endoscope with a radial scan head (UM 96, Olympus/Jap) as sources of distortion. Both instruments were mounted in upright position on the sample holder.

III. RESULTS

A. Undistorted measurements

The precision of the undistorted measurements depends on the distance between the emitter and the detector. At distances of 300 mm and 450 mm, respectively, the deviations never exceeded a value of 0.2 mm, at the far end of the sensitive volume (600 mm) still were below 1 mm. This is in agreement with the specifications.

For the stylus calibration, we found the RMS error to be 4.2 mm in 20 experiments. Figure 5 shows mean value and standard deviation of deviations resulting from undistorted distance measurements. Each distance was measured 10 times. The deviation increases almost linearly with increasing the measured distance.

The effect of sensor orientation is shown in Fig. 6. The deviations are equal to zero when the stylus is rotated ± 20 degrees around the x axis relative to the first measurements. A rotation round the y axis results in relatively constant deviations (average error 3.5 ± 0.9 mm).

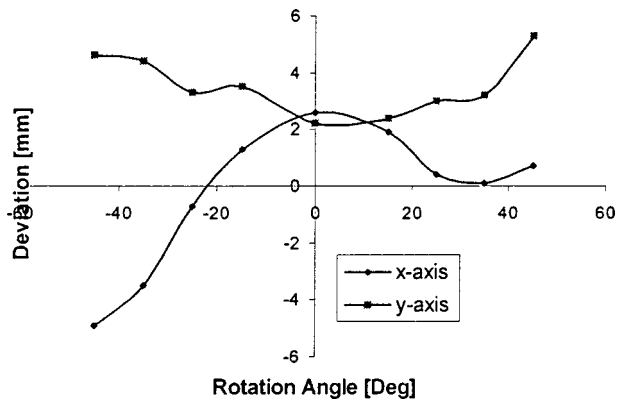


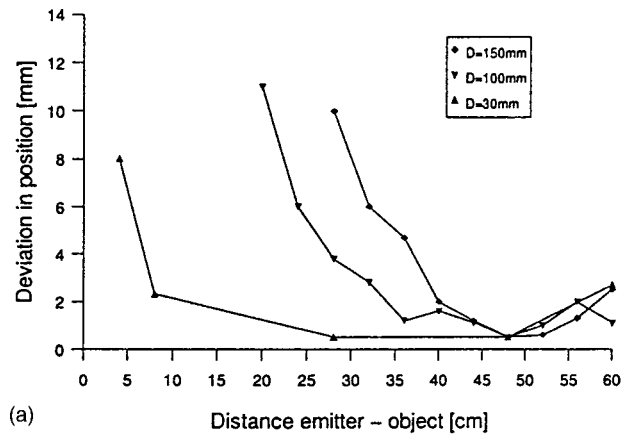
FIG. 6. The effect of sensor orientation on distance measurement obtained with a calibrated stylus. The stylus was rotated by increments of 10 degrees around the x and the y axis, respectively.

B. Influence of wire loops, guiding wires, and optical tracking tools

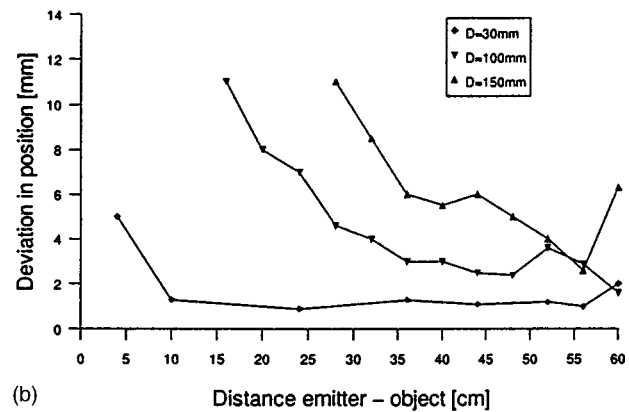
Wire loops: Figs. 7 and 8 show the deviations for a sensor-emitter distance of 600 mm and 300 mm, respectively. The sensor readings exceeded a deviation of 10 mm for loops with diameters greater than 70 mm for distances within 160 mm from the emitter. In contrast, the loop with 30 mm diameter causes negligible distortion. The same objects close to the sensor do not cause large distortions. The extent of the deviation depends on the distance of the object from the emitter and on the distance between emitter and sensor. For each emitter sensor distance there is a zone where sufficient accuracy (<10 mm error) can be obtained. At a distance of 600 mm between emitter and sensor the zone is represented by a distance of 300 mm around the sensor. Moving the sensor to a distance of 300 mm from the emitter results in a reduction of the useful zone to 100 mm at a height of 100 mm. Furthermore, the height of the object characterizing its displacement from the connecting line between emitter and sensor influences the degree of distortion. The effect decreases with increasing displacement. It is evident that the extent of error correlates with the surface area defined by the loop. This is a consequence of the general law of induction.

Wire guides: These tools do not distort the measurements significantly. Because they are isolated, eddy currents do not develop and therefore the resulting magnetic field is much lower than in the case of closed loops so that the resulting distortions could not be distinguished from measurement noise.

Optical tracking sensors: The tested tracking tools were made entirely of titanium or aluminum. Their influence on the accuracy of the position measurements are surprisingly low (Fig. 9). Assuming a tolerable error of 5 mm (as suggested by Zaaroor *et al.*),⁵ an optical tracking sensor can be used satisfactorily anywhere except within a distance of 70 mm to the emitter. It should be noted that the deviations caused when the object is close to the sensor are lower than in all measurements of the other small structures. The results depend significantly on the materials of the different tools.



(a)



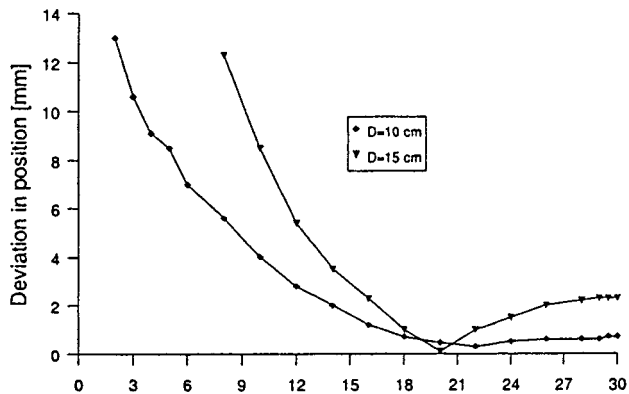
(b)

FIG. 7. Deviations for distance between emitter and sensor of 600 mm, the wire loops are mounted on sample holders at heights of 20 mm and 100 mm, respectively. The x axis is the distance between the wire loop and the emitter. D indicates the diameter of the wire loops.

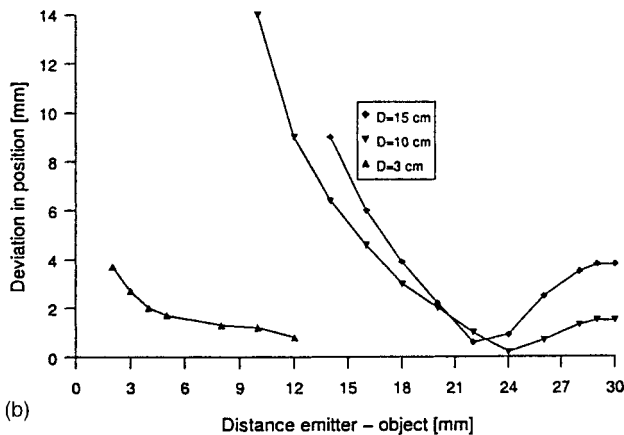
C. Distortions caused by US scan head and a C-arm fluoroscopy unit

US scan head: The distortions resulting from the US scan head depend fundamentally on the way it is mounted on the sample holder (Fig. 10). When the scan head is positioned upright, the distortions are significantly lower than in a horizontal position. This effect can be seen clearly when the scan head is moved close to the sensor. The distortions also increase when the ultrasound machine is switched on.

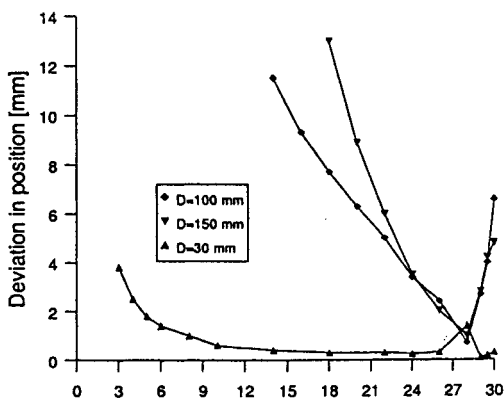
C-arm fluoroscopy unit: The results show that the use of a C-arm unit between the emitter and the sensor during navigation causes severe distortions if either the x-ray tube or the image intensifier tube are close to the emitter (Fig. 11). The distortions are acceptable only when the arm is positioned furthest away from the emitter in our configuration i.e., with $a = -200$ mm [Fig. 11(a)]. The curve obtained for rotation of the C-arm around axis I shows a peak at zero degree [Fig. 11(b)]. In that case, the distance between the x-ray source and the sensor is the closest. For a rotation of the C-arm unit around axis II it can be seen that the worst deviations occur when the image intensifier is close to the emitter (angle=50 degrees, distance emitter—image intensifier=270 mm).



(a) Distance emitter - object [cm]



(b) Distance emitter - object [mm]



(c) Distance emitter - object [cm]

FIG. 8. Deviations for distance between emitter and sensor of 300 mm, the wire loops are mounted on sample holders at heights of 20 mm, 60 mm, and 100 mm, respectively. D indicates the diameter of the wire loops.

D. Distance measurements under distortion

US Scan Head and Endoscope: The resulting deviations, with respect to the scan head, are shown in Fig. 12. The dotted and dashed lines represent the deviation obtained from the distance measurements without objects of distortion (mean value \pm standard deviation). There is no significant difference when the scan head is switched on. In contrast to the measurements shown in Fig. 9, the smallest distance between sensor and scan head is 100 mm when the distance between emitter and scan head is 450 cm in x direction.

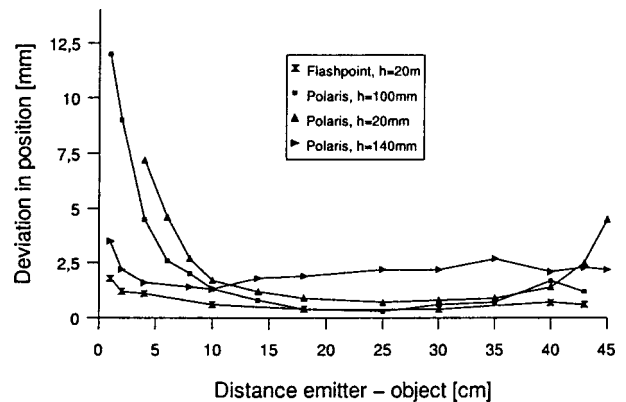


FIG. 9. Deviations for optical tools of two different brands of optical tracking systems and at a distance of 450 mm between emitter and sensor.

The functions resulting from distance measurements obtained when the scan head is mounted upright show the same shape as the functions obtained with the US scan head in an upright position by the simple sensor readings. Referring to the deviations caused from the endoscope (Fig. 13), one can see that the reliability in distance measurement is decreasing when the radial scan head is switched on. All resulting deviations are below 4 mm.

Needle holder, biopsy forceps, and drill handle: These metallic objects, which can be found in operation rooms and interventional suites, can be used during navigation without notable effects (Fig. 14). The measured deviation only slightly exceeds the results from the undistorted measurements. Only the distortions caused by the drill are high when this surgical tool is positioned close to the emitter.

IV. DISCUSSION

The experiments described in this paper give a somewhat ambiguous figure of the performance of this novel tracking system. Overall accuracy was found to be in the range of the manufacturer's specifications, and additional conductive or ferromagnetic do not introduce as significant a deviation as in the case of other commercially available electromagnetic

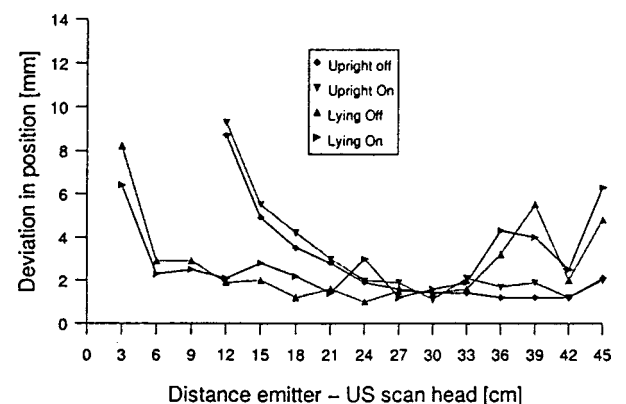


FIG. 10. Deviations caused by a US scan head at a distance of 450 mm between emitter and sensor. The scan head was mounted upright and horizontally. The distortions were recorded under two conditions, when the ultrasound machine was switched on and off.

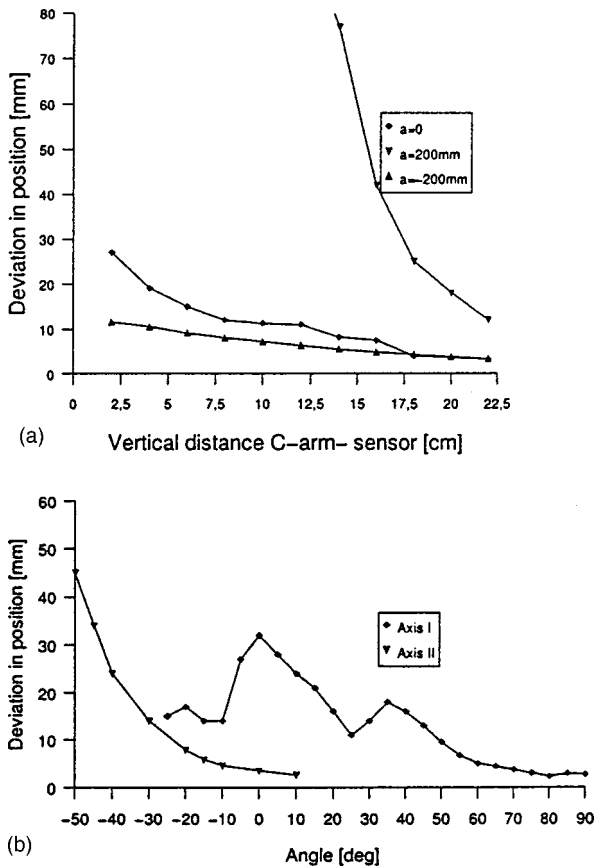


FIG. 11. (a) Distortions for translation of the C-arm fluoroscopy unit in vertical direction for three different horizontal distances between the C-arm and the sensor. A positive a means a horizontal shift towards the emitter. $a=0$ means that the x-ray source is positioned exactly below the sensor. Axis I in (b) defines an orbital movement of the C-arm where a positive angle refers to the motion of the x-ray source towards the emitter. Axis II specifies the angulation movement of the C-arm unit. Positive values of the angles refer to the movement of the image intensifier of the C-arm towards the emitter.

trackers tested under similar conditions.⁸ Based on our results, it is to be assumed that the errors from interfering objects can be kept at a reasonably small level in many clinical applications if it can be made sure that some simple con-

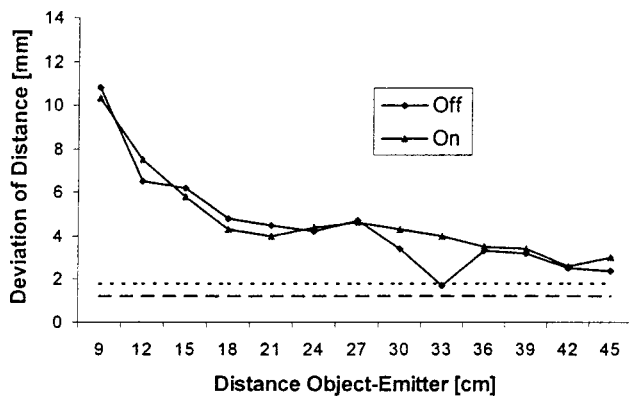


FIG. 12. Deviations in distance measurements resulting from the US scan head. The dotted line represents the mean value of the undistorted distance measurements at 20 cm plus the resulting standard deviation. The dashed line is calculated from the mean value minus the standard deviation.

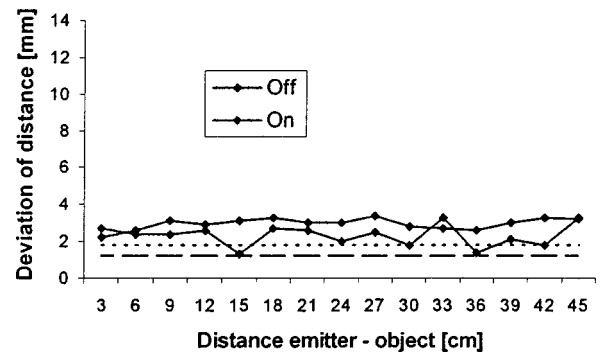


FIG. 13. Deviations in distance measurements for the endoscope. All deviations are below 4 mm. The dashed and dotted lines result from the undistorted distance measurements (mean \pm standard deviation).

straints are respected. For instance, the use of guiding wires would not lead to notable distortions as measured for conducting wire loops due to the impossibility of forming a closed loop, thus avoiding secondary magnetic fields. Similarly, US scan heads should be used near to the sensor, not the emitter. The C-arm, however, forms an exception from this rule, and it is definitely necessary to find a way to overcome this restriction by further technological development of the tracker. Furthermore, a solution has to be found to overcome the limitations caused by the small sensitive volume. One possible approach is to design a hybrid tracking system,² using an additional optical tracking tool to monitor displacements of the emitter.

Information about all six degrees of freedom of a tracked flexible instrument would require the use of two 5 degree-of-freedom sensors, mounted in an arbitrary but fixed position on the instrument. Northern Digital offers 6 degree-of-freedom sensors which consist of two 5 degree-of-freedom sensors mounted perpendicular in a plastic case. Unfortunately, this sensor was not available for our experiments, and the evaluation of such a probe for a specific clinical applications should form the background for further work in the field of digitizer assessment for image guided therapy. As an intermediate solution, we have used two sensors mounted to an endoscope's tip for calibration of an endosonographic scan head. Nevertheless, the 5 degree-of-freedom probe can

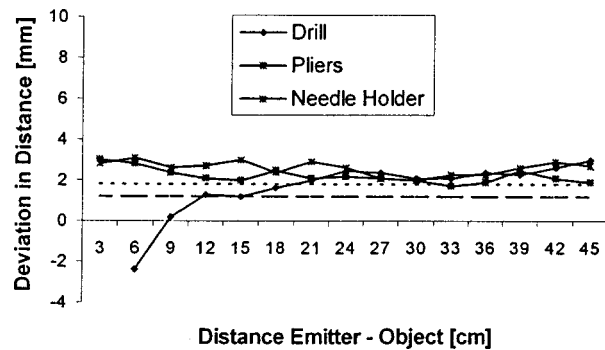


FIG. 14. Deviation in distance measurements for various medical tools. These tools can be seen in Fig. 3. The dashed and dotted lines are obtained by the mean \pm standard deviation of the undistorted distance measurements.

be used for a wide variety of applications. For instance, only one sensor is required to monitor the position of an instrument that is coaxial to sensor's main axis.

V. CONCLUSIONS

The further growth of image guided therapy is vitally dependent on the development of innovative applications offering significant clinical benefit for widespread medical procedures. Tracking minimally invasive instruments is a key technology to pursue this goal. The tracker evaluated in this paper is a step towards it.

However, the assessment of inaccuracies in position measurements with magnetic trackers induced by metallic materials resulted in a wide range of distortion values, with clear indications which geometric configurations should minimize inaccuracies. Still it is necessary to avoid configurations during a medical procedure which are known to produce intolerable distortions, and this is definitely a major problem for real-life application in medicine. In particular, it is unlikely that the clinical environment can be significantly adopted for the sole purpose of using an electromagnetic tracking system. In spite of occasionally large distortions it seems to be evident that this tracking system offers many possibilities for new applications of CAS and interventional therapy.

ACKNOWLEDGMENTS

This project was supported by the Jubiläumsfonds der Österreichischen Nationalbank OeNB #8450. W. Birkfellner is supported by the Swiss National Foundation SNF-Grant "Computer Aided and Image Guided Medical Interventions CO-ME."

^{a)}Electronic mail: Jhummel@gmx.at

^{b)}Also at Ludwig-Boltzmann Institute of Nuclear Medicine, Vienna, Australia.

¹R. B. Metson, M. J. Cosenza, M. J. Cunningham, and G. W. Randolph, "Physician experience with an optical image guidance system for sinus surgery," *Laryngoscope* **110**, 972–976 (2000).

²W. Birkfellner, F. Watzinger, F. Wanschitz, R. Ewers, and H. Bergmann,

"Calibration of tracking systems in a surgical environment," *IEEE Trans. Med. Imaging* **17**, 737–742 (1998).

³R. Hauser, B. Westermann, and R. Probst, "Noninvasive tracking of patient's head movements during computer-assisted intranasal microscopic surgery," *Laryngoscope* **107**, 491–499 (1997).

⁴H. W. Schroeder, W. Wagner, W. Tschiltshcke, and M. R. Gaab, "Frameless neuronavigation in intracranial endoscopic neurosurgery," *J. Multi-variate Anal.* **94**, 72–79 (2001).

⁵M. Zaaroor, Y. Bejerano, Z. Weinfeld, and S. Ben-Haim, "Novel magnetic technology for intraoperative intracranial frameless navigation: in vivo and in vitro results," *Neurosurgery* **48**, 1100–1107 (2001).

⁶A. R. Javer, F. A. Kuhn, and D. Smith, "Stereotactic computer-assisted navigational sinus surgery: accuracy of an electromagnetic tracking system with the tissue debrider and when utilizing different headsets for the same patient," *Am. J. Rhinol.* **14**, 361–365 (2000).

⁷J. Hummel, W. Birkfellner, M. Figl, R. Hanel, and H. Bergmann, "Laboratory assessment of a Miniature Electromagnetic Tracker," *Proc. SPIE* **4681**, 94–99 (2002).

⁸W. Birkfellner, F. Watzinger, F. Wanschitz, G. Enislidis, C. Kollmann, D. Rafolt, R. Nowotny, R. Ewers, and H. Bergmann, "Systematic distortions in magnetic position digitizers," *Med. Phys.* **25**, 2242–2248 (1998).

⁹J. J. Stone, B. L. Currier, G. L. Niebur, and K. N. An, "The use of a direct current electromagnetic tracking device in a metallic environment," *Biomed. Sci. Instrum.* **32**, 305–311 (1996).

¹⁰J. S. Day, D. J. Murdoch, and G. A. Dumas, "Calibration of position and angular data from a magnetic tracking device," *J. Biomech.* **33**, 1039–1045 (2000).

¹¹M. Nakamoto, Y. Sato, Y. Tamaki, H. Nagano, M. Miyamoto, T. Sasama, M. Monden, and S. Tamura, *Magneto-Optic Hybrid 3-D Sensor for Surgical Navigation*, MICCAI 2000 (Springer, New York, 1935), pp. 839–848.

¹²S. B. Solomon, P. White, Jr., C. M. Wiener, J. B. Orens, and K. P. Wang, "Three-dimensional CT-guided bronchoscopy with a real-time electromagnetic position sensor: a comparison of two image registration methods," *Chest* **118**, 1783–1787 (2000).

¹³O. H. Gilja, T. Hausken, S. Olafsson, K. Matre, and S. Odegaard, "In vitro evaluation of three-dimensional ultrasonography based on magnetic scanhead tracking," *Ultrasound Med. Biol.* **24**, 1161–1167 (1998).

¹⁴N. deGroot, "3-dimensional catheter positioning during radiofrequency ablation in patients," *J. Cardiovasc. Electrophysiol.* **11**, 1183–1192 (2000).

¹⁵N. J. Hopf, P. Grunert, K. Darabi, C. Busert, and M. Bettag, "Frameless neuronavigation applied to endoscopic neurosurgery," *Minim. Invasive Neurosurg.* **42**, 187–193 (1999).

¹⁶A. Hartov, S. D. Eisner, M. S. David, W. Roberts, K. D. Paulsen, B. S. Platenik, and M. I. Miga, "Error analysis for a free-hand three-dimensional ultrasound system for neuronavigation," *Neurosurgical, Focus* **6**, 5 (1999).